Sustainable Structures
ISSN: 2789-3111 (Print); ISSN: 2789-312X (Online)
http://www.sustain-dpl.com/journal/sust
DOI: 10.54113/j.sust.2025.000073

ORIGINAL ARTICLE

Analysis of mechanical properties of fly ash and boiler slag integrated geopolymer composites

Jasim Ahmed Chowdhury[a], Md. Shahidul Islam[a], Md. Ashraful Islam[a, *], Md Abdullah Al Bari[b, c], Arup Kumar Debnath[a]

[a]Department of Mechanical Engineering, Khulna University of Engineering & Technology, Khulna, Bangladesh
[b]Department of Mechanical Engineering, King Fahd University of Petroleum & Minerals, Dhahran, 31261, Saudi Arabia
[c]Interdisciplinary Research Center for Sustainable Energy Systems, King Fahd University of Petroleum & Minerals, Dhahran 31261, Saudi Arabia
[*]Corresponding Author: Md. Ashraful Islam.   Email: md.islam@me.kuet.ac.bd

Abstract: This study explores sustainable alternatives to conventional raw materials in composite manufacturing by integrating fly ash (FA) and boiler slag (BS) into geopolymer composites. FA and BS were combined with alkali activators (AA) to evaluate their mechanical and physical properties under varying compositions and curing conditions. From bottom ash, only the boiler slag portion was selected for use in this study, which was ground to 300 μm particle size. The research examined the effects of BS content (25%, 50%, and 75%), solid-to-liquid ratios (0.5, 1.0, 1.5, and 2.0), AA ratios (Na_2SiO_3/NaOH: 1.0 to 2.5), and curing temperatures (60 ℃ to 90 ℃) on the compression strength of the composites. Results showed that composites with 25% BS and an AA ratio of 1.5 achieved the highest compressive strength (30.38 MPa) after 7 days of curing. Apparent porosity and water absorption decreased with increasing BS content, while optimal curing temperatures ranged from 70 ℃ to 80 ℃. At elevated temperatures, compressive strength declined due to thermal degradation, but composites maintained the performance comparable to conventional materials. SEM analysis revealed a geopolymer matrix with dense microstructures. These findings demonstrate that incorporating BS and FA into composite manufacturing provides a viable eco-friendly alternative to traditional materials, reducing reliance on geo-sand and cement while enhancing sustainability.

Keywords: Fly ash, bottom ash, boiler slag, alkali-activator, geopolymer composites.

1 Introduction

Fly ash (FA) is an excellent alternative to traditional clay bricks, which offers a sustainable solution by conserving valuable clay resources and protecting agricultural land from depletion [1]. The production of FA is rapidly growing in the current industrial environment; in 2024, the overall market was valued at approximately USD 13.5 billion [2]. With the growing financial market size of FA, the fly ash brick (FAB) industry is also scaling up, transforming into a multi-million-dollar sector [3, 4]. The traditional process of manufacturing FAB frequently uses cement and geo sand [5], which has negative impact on the

Received: 2 December 2024; Received in revised form: 15 February 2025; Accepted: 2 May 2025

environment by disrupting the ecosystem, also increasing carbon emissions [6]. To alleviate these environmental issues, substituting sand with boiler slag offers an economical and eco-friendly solution, which can be reused as a valuable resource [7]. Also, replacing cement with alkali activators (AA) through the polymerization process offers a promising solution for the construction industry [8].

The chemical process by which alkali activators (sodium or potassium hydroxide mixed with silicates) react with aluminosilicate materials (such as FA, slag, or kaolinite) to form a geopolymeric materials is known as geopolymerization. Geopolymerization process is not only environmentally friendly but also energy-efficient, requiring only moderate energy inputs compared to traditional cement production. As a result, geopolymers offer a sustainable and eco-conscious alternative for construction and other industrial applications [9]. The process of Portland cement production generates lots of CO_2 along with other harmful pollutants to the environment. Studies found that one ton of Portland cement production requires approximately 2.8 tons of raw materials, which results in emission of 6000-14000 m^3 of dust-laden air, containing 0.7 to 800 g/ m^3 of dust. Additionally, this process also releases approximately one ton of CO_2 [9]. Cement production is responsible for approximately 5–7% of global CO_2 emissions [10]. This CO_2 is primarily produced due to the decarbonization of limestone in the kiln during cement manufacturing [11].

On the other hand, geopolymers have emerged as a potential solution for utilizing by-products in an environmentally friendly way. They offer diverse applications, including the manufacturing of precast structures, non-structural components, concrete pavements, and other concrete products, while also immobilizing toxic waste and providing resistance to heat and harsh environments [11, 12]. Divya Khale et. al [9] state that geopolymers are alumino-silicate materials formed through polymerization, where tetrahedral silica and alumina units interlink, stabilized by alkali cations like Na, K, or Ca. Alkali hydroxides or salts dissolve silica and alumina from source materials, facilitating the formation of a reactive gel that hardens into an amorphous to semi-crystalline structure. Unlike zeolites, geopolymers do not crystallize fully and form in open systems. The addition of pozzolans enhances properties like durability, strength, and thermal stability, though strength development can be gradual. The final structure and leaching characteristics depend on cation incorporation and the reaction environment, distinguishing geopolymers from zeolites in composition and formation. From typical alumino-silicate reaction [8, 9] it can be noticed that no carbon emissions or harmful environmental by-products are produced, making geopolymerization an environmentally safe process.

One of the sources of FA is from coal-fired power generation plants. In 2023, approximately 10,468 TWh of electricity was generated using coal globally [13], consuming nearly 8.54 billion tons of coal. Although, there is a decline in coal consumption in advanced economies like the U.S. and the EU as they are very focused on using green and renewable energy, but it increased in Asia, especially India and China where the demand for electricity surged [14]. In Bangladesh, several coal-based power plants are now operational, producing 7,179 MW of electricity and accounting for 25.79% of the country’s total power generation [15].

Combustion of coal generates many wastes and byproducts among which two major byproducts are fly ash (FA) and bottom ash (BA) [7]. As per the report of 2023, American coal ash association [16] approximately 28,227,974 Tons of FA and 7,576,840 Tons of BA were produced in 2022. Both byproducts are produced from coal ash. Coal ash is a eutectic mixture of silicon dioxide (SiO_2), aluminum oxide (Al_2O_3), iron oxide (Fe_2O_3), calcium oxide (CaO), magnesium oxide (MgO), titanium dioxide (TiO_2), sodium oxide (Na_2O), potassium oxide (K_2O), phosphorus pentoxide (P_2O_5), trace elements like arsenic (As), chromium (Cr), lead (Pb), mercury (Hg), sulfur compounds (e.g., sulfates) and unburnt carbon. BA encompasses boiler slag (BS), heavy particle fly ash and other industrial impurities. Boiler slag is produced by the melting of coal ash during combustion [17, 18] This melting occurs when the boiler coal combustion temperature goes beyond the melting point temperature of the eutectic melting point of the ash mixture. In a typical coal-based thermal power plant, initially, coal is transported from the coal stockyard to the coal bunker and then to the coal mill, where it is ground into fine powder before being fed into the furnace for coal combustion. During the coal combustion process, various minerals and impurities present in the coal are released into the boiler furnace as ash particles. Some particles are carried by the flue gas, and the rest of the coarse materials are settled at the bottom of the furnace. These heavy, coarse materials, commonly referred to boiler slag (BS), [17]. The lighter particles pass through the furnace to the second pass of the boiler and then into the Electrostatic Precipitator (ESP). The ESP collects these lighter particles with the help of high-voltage flue gas ionization, referred to as FA, and stores them in the ESP Hopper [19].

According to Coal combustion products (CCPs) worldwide [16], approximately 47% of the BS generated in 2022 was utilized in various industries and applications. Reflecting its growing use in construction, road stabilization, and other sectors. Blasting grit remains the most widely utilized application of BS, but it poses significant environmental concerns due to its contribution to air pollution through dust generation. The cement industry is the second largest user of BS in its production operations; nonetheless, this practice has disadvantages, particularly with carbon emissions. In contrast, the concrete industry utilizes BS far less than these two sectors, highlighting a disparity in its applications and environmental impact.

In fly ash bricks (FAB), sand primarily acts as a filler, supporting FA and binding materials such as cement or alkali activators (AA) [20]. The absence of suitable fillers can lead to issues like increased porosity, reduced mechanical strength, and higher water absorption [21]. Given its pozzolanic properties, boiler slag (BS) has the potential to replace sand, serving as an effective filler material in FAB manufacturing.

While previous research has explored the use of bottom ash (BA) in combination with FA, studies focusing exclusively on BS with alkali activators remain limited. For instance, Mahdi Rafieizonooz et al. [7] demonstrated that replacing sand with fine BA and cement with FA improved concrete strength and reduced shrinkage. Similarly, S. Naganathan et al. [22] developed self-compacting mixtures incorporating FA, BA, and cement for brick production, achieving performance comparable to conventional clay bricks. Djwantoro Hardjito et al. [23] also observed that substituting 50% of the sand with BA reduced the water demand in concrete mixtures.

The AA ratio is another critical parameter influencing the strength of composite materials and has been widely studied [24, 25]. H. Y. Leong et al. [26] investigated the effect of different hydroxide-to-silicate ratios using three types of hydroxides—sodium, potassium, and calcium. Their findings showed that sodium- and potassium-based hydroxides produced the most favorable results. In this study, sodium hydroxide (NaOH) was selected as the primary activator, and the effects of varying the Na_2SiO_3/NaOH ratio were examined.

As, the AA weight ratio significantly impacts composite performance. Previous studies have reported a range of variations in this ratio—1.43, 1.67, 2, and 2.5—when working with fly ash-based composites [27, 28]. These differences contribute to variations in the mechanical and durability properties of the final material.

Considering the gaps identified in prior research on the development of composites using BS, FA, and alkali activators. Subsequently, variations in BS content (25%, 50%, and 75%), solid-to-liquid ratios (0.5, 1, 1.5 and 2.0), and alkali activator ratios (Na2SiO3/NaOH: 1.0, 1.5, 2.0, and 2.5) were examined under 24-hour curing at 70 ℃, followed by ambient curing. Finally, the best-performing mix was further analyzed for flexural strength, porosity, and the effects of curing temperature (60 ℃, 70 ℃, 80 ℃), thermal exposure (200 ℃, 400 ℃, 600 ℃, 800 ℃) and duration (7 days and 28 days).

2 Materials and Methods

2.1 Raw Materials

FA and BS were sourced from the 1320 MW Maitree Thermal Super Power Plant in Rampal, Bangladesh. During the collection process, it was verified that the FA (**Fig. 1.a**) was free from visible foreign materials such as steel, mud, and plastic. FA was collected as a fine powder. On the other hand, the BS, characterized by its hard, dense, black appearance and rough, porous surface texture, was collected as a chunk shown in **Fig. 1. (b-c)**. BS was grounded to a particle size below 300 microns (**Fig. 1.d**). It was sieved to ensure the particle size met the desired specification. FA (**Fig. 1.e**) & BS (**Fig. 1f**) particle distribution can also be observed in the SEM images.

Sodium silicate was sourced from Silica Solution BD, Bangladesh and the composition was labeled as 8.23% Na_2O, 29.77% SiO_2 and 62.0% H_2O.

Sodium hydroxide was collected as pellets sourced from Merck, Germany, were utilized. The sodium hydroxide pellets boasted an assay of ≥ 97.0% and M=40 g/mol, indicating a high purity level. Minimal impurities such as carbonate (as Na_2CO_3) at ≤ 1.0%, chloride (Cl) at ≤ 0.012%, and sulfate (SO_4) at ≤ 0.010% were presented.

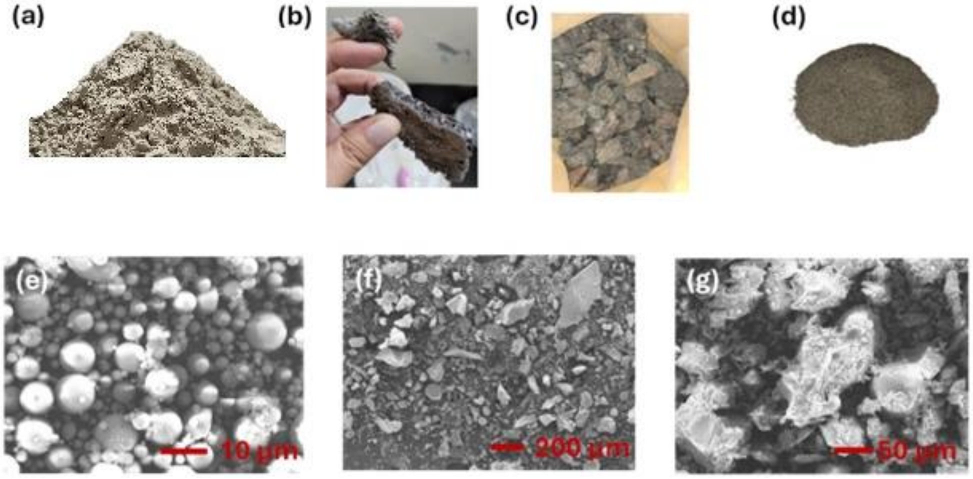

Fig. 1 (a)Fly ash (b-c) Boiler Slag (as received) (d) Boiler Slag (after grinding) (e) Fly-Ash SEM Image @10 µm (f) BS SEM Image @200 µm (g) @ 50 µm

2.1.1 Fly Ash (FA) Composition

The identification of the appropriate FA composition is crucial for this research. As a key bonding material, FA impacts the composite's performance. Various samples are thoroughly examined to find the best properties that align with ASTM-C618-22. This meticulous selection ensures the composite material's coherence and efficacy, laying a strong foundation for the research. The detailed elemental composition data obtained from Energy-Dispersive X-ray Spectroscopy (EDS) analysis for these samples can be found in **Table 1**. From the analysis, it is evident that they belong to the F-class FA category, but according to ASTM C618-22 and O. Juntarasakul [29] a higher combined content of SiO_2, Al_2O_3, and Fe_2O_3 enhances the quality of FA, making it more suitable for concrete applications by improving its pozzolanic properties. FA was used for this study is appearing remarkable values for of SiO_2, Al_2O_3, and Fe_2O_3.

Table 1. Comparison of Current Study & ASTM-C618-22 Standard Results of EDS Mass%

Elemental Composition	SiO_2	CaO	Fe_2O_3	Total	SO_3	Al_2O_3	SiO_2/Al_2O_3
ASTM-C618-22	For F Class Fly Ash, Silicon dioxide (SiO_2) + aluminum oxide (Al_2O_3) + Iron oxide (Fe_2O_3), min, 50%				18% max	5% max	-
Current Study	53.11	23.22	10.75	87.08	8.45	-	2.29

2.1.2 Boiler Slag (BS) Composition

In this study large granular size BS had been ground to a size below 300 microns, which aligns with the particle size of conventional fine grain size river geo-sand. The EDS report on **Table 2** shows that FA and BS have same kind of chemical elements.

Table 2. Boiler Slag EDS Analysis Results

Element	**Na_2O**	**MgO**	**Al_2O_3**	**SiO_2**	**CaO**	**FeO**	**SiO_2/Al_2O_3**
Mass%	1.54	1.69	15.28	58.14	4.11	11.44	3.80

2.2 Composite Preparation

In this study, all the solid raw materials, i.e., FA and BS, were collected from Bangladesh-India Friendship Power Company Limited (BIFPCL). The total fabrication process can be highlighted below in **Fig. 2**.

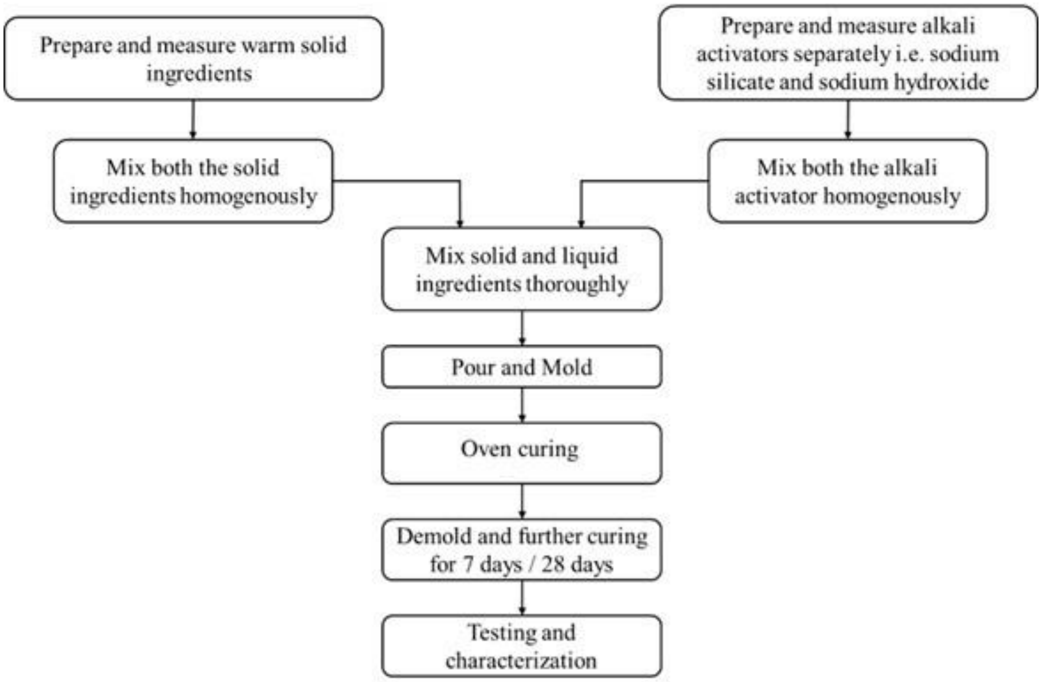

Fig. 2. Flow chart of geopolymer composite making

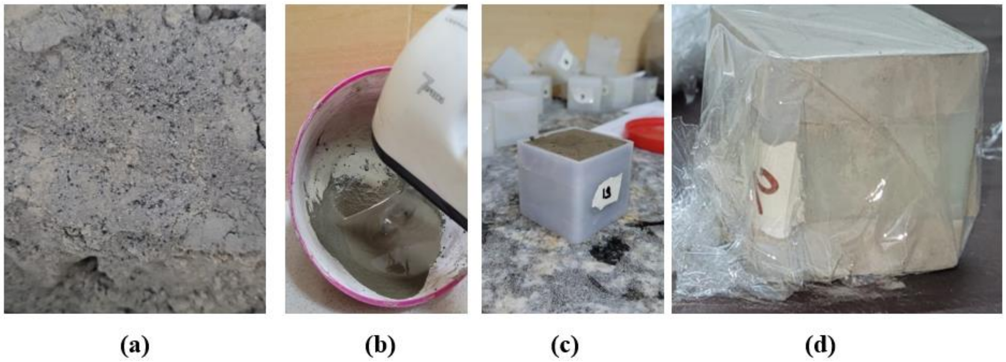

Fig. 2. (a) Mixing of solid particles-final mixture of boiler slag and fly-ash; (b) Mixing both solid and liquid particles with the help of handheld mixer machine; (c) Final Mold Preparation; (d) Polyvinyl Paper Wrapping

The process starts with the FA that is put in an oven set to 110 ℃ for 24 hours. After the heating period, the ash's temperature and weight were measured again to calculate how much moisture was in the initial FA. During the preparation of the composite, the FA was kept warm using a small induction oven (@above 100 ℃) to maintain its condition. An initial grinding was performed using a grinding machine to achieve finer particles for the BS. A sieve was done (sieve size 50) to ensure the particle size remained below 300 microns of BS. After all the solid ingredients were prepared, their weights were meticulously measured on a weight scale to match the required specifications for preparing the composite material. Then, BS and FA were mixed thoroughly until a uniform consistency was achieved **Fig. 2(a).**

The sodium hydroxide solution was prepared 24 hours before composite fabrication. Sodium hydroxide is mixed with sodium silicate according to the specified requirements. Mixing was continued until noticeable heat generation was observed, indicating the initiation of the reaction. After finalizing the solid and liquid components, they were weighed on a pan as required. The components are then thoroughly mixed using a handheld mixer machine until a homogeneous mixture paste was achieved **Fig. 2(b)**. After getting the paste, it was poured into the silicon mold **Fig. 2(c).** Polyvinyl paper **Fig. 2(d)** has been used over the mold at initial stage. After the mold preparation, samples had been cured in oven and environment as required.

2.3 Composites Characterization

Compression tests were carried out using 50×50×50 mm cubic samples prepared as per ASTM-C109 [30]. The flexural strength test, conducted by ASTM C78 [31] standard, evaluates the bending behavior of geopolymer composites. Samples were 160×40×40 mm with a 100 mm span length. Both compressive and flexural tests were conducted using the Shimadzu AGX V 300kN Universal Testing Machine (UTM) applying ASTM C109 standard protocol. The reported compressive strength was the average of the three tests. Porosity had been conducted under the ASTM testing standard C373 [32]. Samples undergoing thermal exposure were heated in a furnace on the sixth day, with the temperature increasing at a rate of 10 ℃ per minute from room temperature. Once the target temperature was reached, it was maintained for three hours. The samples were then allowed to cool naturally within the furnace until they returned to room temperature. Compression testing was conducted the following day [23].

2.4 Variations

The strength of composites produced through polymerization depends on several factors, including the percentage of aluminosilicate materials [33, 34] hydroxide molarity [24, 27] curing temperature [35, 36] and duration [28] among others.

The current study initially aimed to validate the compressive strength performance of the FA by comparing it with results from similar previous studies [24], [37], [38]. Varying weight percentages of BS were mixed with different AA ratios while maintaining a fixed solid to liquid ratio i.e. 2. This process evaluated compressive strength and flexural stress. Based on the optimal composition identified through compressive strength analysis, further investigations explored the impact of varying solid to liquid weight ratios (solid means FA and BS mixer, liquid means AA). Finally, the study examined the effect of BS content on compressive strength, NaOH concentration variation, porosity, thermal exposure, as well as the influence of different curing temperatures and durations. For each variation three samples were prepared, and midpoint value was taken into consideration. The standard deviation was maintained below 5%.

3 Results and discussions

3.1 Fly-Ash Analysis

Table 3. For Fly-Ash composites

Parameter	Details
Composition	100% Fly Ash (FA), No Boiler Slag (BS)
AA Ratio (Na_2SiO_3 /NaOH)	1, 1.5, 2, 2.5
Solid-to-Liquid Ratio	2

For an initial assessment, the compressive strength of the fly-ash composite was investigated, and the results were compared with the available findings in different literature. The compressive strength performance at varying alkali activator ratios was shown in **Fig.4**. The mix ratio of different composites used in **Fig.4** was provided in **Table 3**. The results of the present study were consistently found to have outperformed those reported by Morsy et al. [38] and Pavithra et al. [37] across all tested AA ratios. Although better results were achieved by Abdullah et al. [24] at an AA ratio of 2.5, their findings still fell short of the highest result observed in this study, which was attained at an AA ratio of 1. This highlighted the superior efficacy of the fly ash formulations and methodologies employed in the current research.

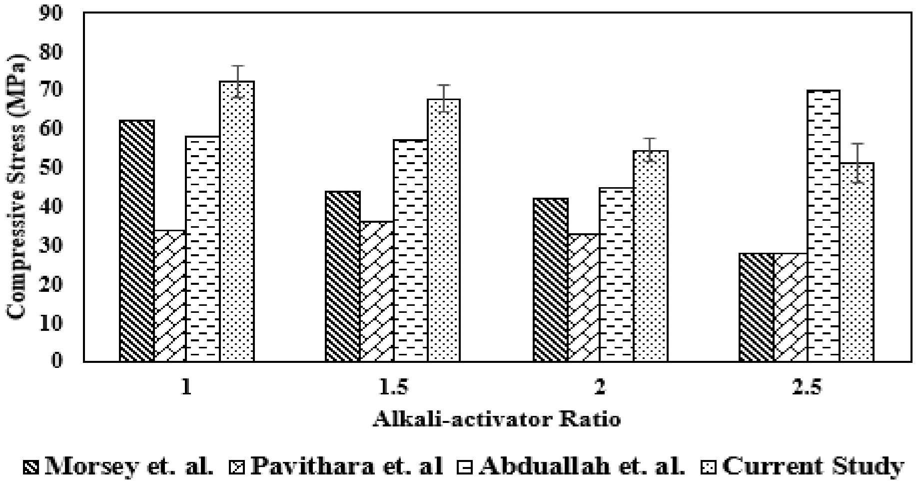

Fig. 3. Comparison of Current Study and Previous Study Results of Composites Made with 100% FA

3.2 FA & BA Composites

3.2.1 Apparent Porosity and Water Absorption Test

From **Table 4**, the actual density and bulk density is consistently higher for BS comparing with FA. This also indicated that BS is heavier than FA. Which has a direct impact of weight with those composites which has more *wt*% of BS.

Table 4. Physical and mechanical properties of geopolymers

Actual Density		Bulk Density	
FA	**BS**	**FA**	**BS**
1926.34 kg/m^3	2108.35 kg/m^3	1540 kg/m^3	1600 kg/m^3

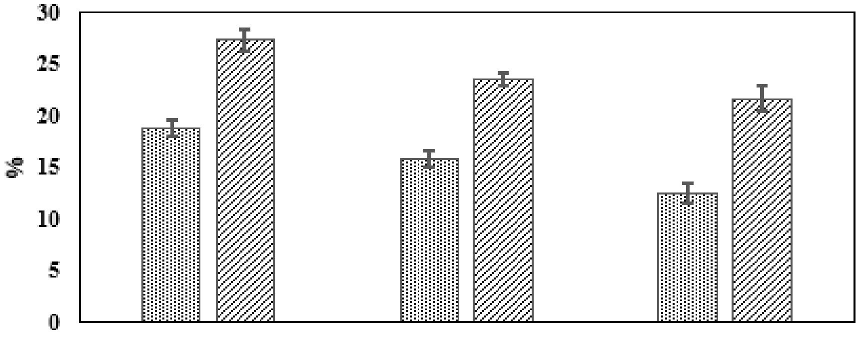

Fig. 4 Percentage of BS Vs Percentage of Water Absorption & Apparent Porosity

For the apparent porosity and water absorption test, the variation was followed as mentioned on **Table 5**. From the **Fig.5**, as the proportion of BS increases from 25% to 75%, both water absorption and apparent porosity show a decreasing trend, indicating a denser and less porous structure. At each composition level, apparent porosity remains higher than water absorption, which is expected since porosity accounts for total void space, while water absorption considers only the retained water. The lowest values for both properties are observed at 75% BS, suggesting that a higher BS content enhances the compactness and reduces permeability in the composite. This trend implies that Boiler Slag (BS) improves the material's structural integrity by minimizing voids, making it more suitable for applications requiring reduced water absorption and higher density.

Table 5. For Apparent Porosity, Water Absorption and Thermal Exposure Test

Parameter	Details
Composition	BS: FA Ratios- 25:75, 50:50, and 75:25.
AA Ratio (Na_2SiO_3 /NaOH)	1.5
Solid-to-Liquid Ratio	1.5

3.2.2 Compressive & Flexural Strength Analysis:

Based on the composition detailed in **Table 6**, the composites were produced, and the results are shown in **Fig.6.** It can be observed that the optimum alkali activator (AA) ratio is 1.5, at which the highest compressive strength, approximately 30.38±4 MPa, is achieved for 25% BS content. Beyond this point, increasing the AA ratio leads to a decline in compressive strength.

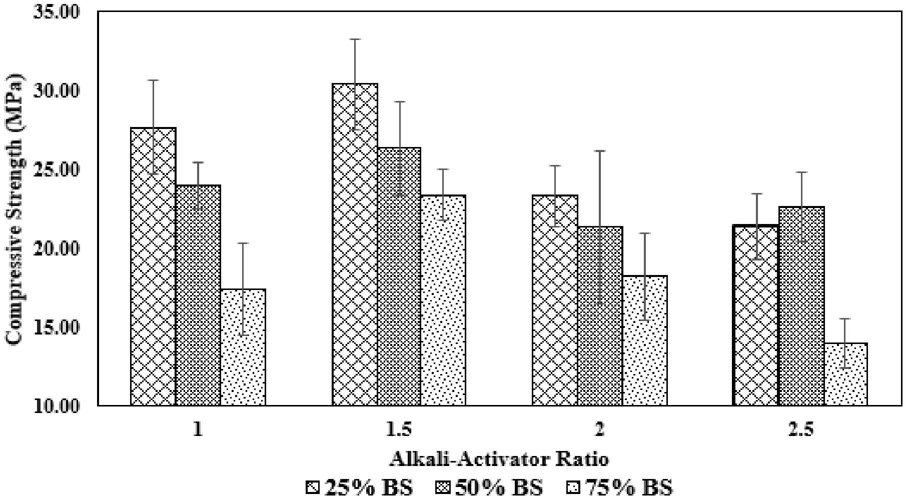

Fig. 5 Compressive strength with various sodium silicate/10 M NaOH ratios with BS *wt*% variation

Table 6. FA & BA Mixing Proportion Variation

Parameter	Details
Composition	BS: FA Ratios- 25:75, 50:50, and 75:25.
AA Ratio (Na_2SiO_3 /NaOH)	1, 1.5, 2, 2.5
Solid-to-Liquid Ratio	2

Additionally, increasing the BS percentage generally reduces the compressive strength of the composite, except at an AA ratio of 2.5, where the 50% BS composite exhibits higher compressive strength compared to the 25% and 75% BS composites. However, when compared to the 100% FA composite, the compressive strength decreases by approximately 55.15% at a similar AA ratio due to the incorporation of BS. A continuous fall of compressive strength can be seen with increasing rate of BS *wt*%. This reduction in strength can likely be attributed to the lower pozzolanic activity of BS compared to FA.

Fig. 6 illustrates a declining trend in flexural strength as the weight percentages of alkali activator and BS increase. This indicates that with the increasing rate of BS the composites appear weak internal bonding and particle packing. Moreover, AC 125 exhibits lower strength compared to AC 225, possibly due to the availability of alkaline activators (AA) required for the chemical reaction with fly ash (FA) and boiler slag (BS), which depends on the applied *wt*% of AA. Since AC 225 contains a higher concentration of NaOH solution than AC 125, this could also contribute to the difference, with AC 225 achieving the highest strength at the optimum NaOH *wt*%.

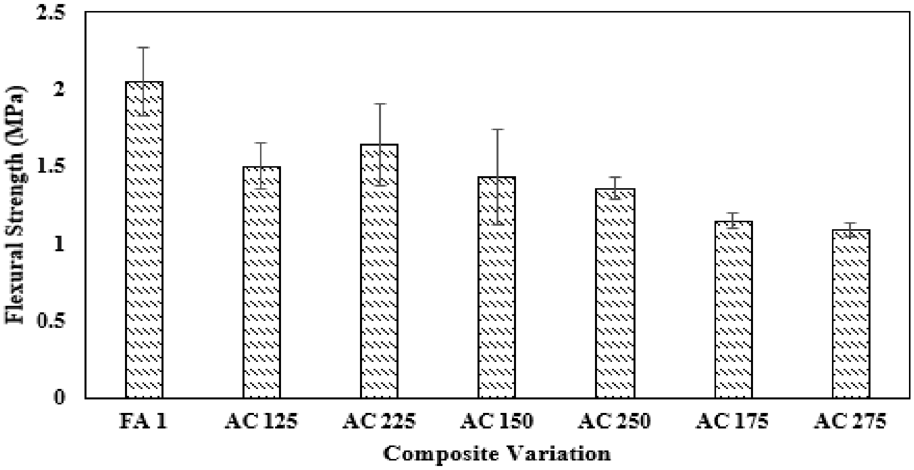

Fig. 6 Flexural strength for various sodium silicate/ NaOH ratios with BS wt% variation

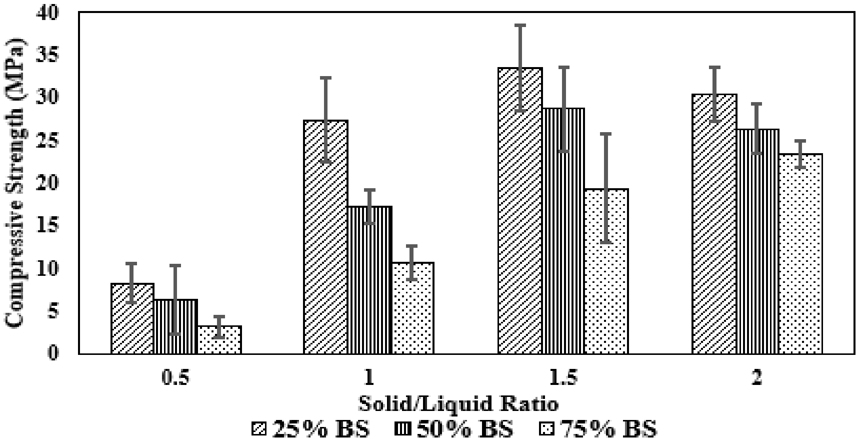

Fig. 7 Strength of Composite with Different Solid to Liquid Ratio

3.2.3 Solid to Liquid Ratio:

It was noted that the impact of the AA ratio and BS ratio on the composites had been examined while maintaining a fixed solid to liquid (*S*/*L*) ratio of 2. Moving forward, the intention was to investigate how variations in the *S*/*L* ratio influence compressive strength. The composition outlined in **Table 7** was used for the *S*/*L* ratio variation tests, with ratios ranging from 0.5 to 2.0.

Table 7. Solid to Liquid Ratio Variation

Parameter	Details
Composition	BS: FA Ratios- 25:75
AA Ratio (Na_2SiO_3 /NaOH)	1, 1.5, 2, 2.5
Solid-to-Liquid Ratio	0.5, 1, 1.5, 2.0

From the **Fig. 7**, it is evident that compressive strength increases gradually up to a ratio of 1.5 but declines beyond this point. Additionally, at a ratio of 0.5, the strength was notably low, attributed to an excess of alkali activator in the mixture which was not entirely dissolving and forming a sticky layer on the surface of the composite. At *S*/*L* 2, the reduction in strength could be attributed to excessive water, as excess of water does influence the composite's structural integrity [39].

3.2.4 NaOH Concentration Variation:

In the current study, compressive strength analysis was conducted using the compositions detailed in **Table 9.** The concentration of the alkali solution was varied between 8M and 14M by adjusting the water content. The results, presented in **Fig. 8**, indicate that compressive strength increased steadily from 8M to 12M. This increase can be attributed to the higher NaOH concentration, which enhances the leaching of silica and alumina, increases the Na_2O/Al_2O_3 ratio, and introduces more Na ions. These factors collectively Balance charges and promote the formation of an aluminosilicate network during geopolymerization [40, 41].

Table 8. NaOH Concentration Variation

Parameter	Details
Composition	BS: FA Ratios- 25:75, 50:50, and 75:25.
AA Ratio (Na_2SiO_3 /NaOH)	1.5
Solid-to-Liquid Ratio	1.5
NaOH Concentration	8, 10, 12, 14

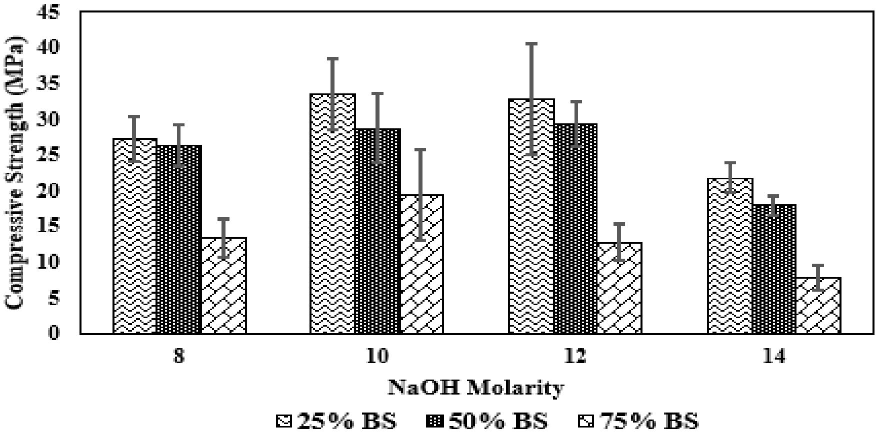

Fig. 8 Strength of Composite with Different NaOH Concentration.

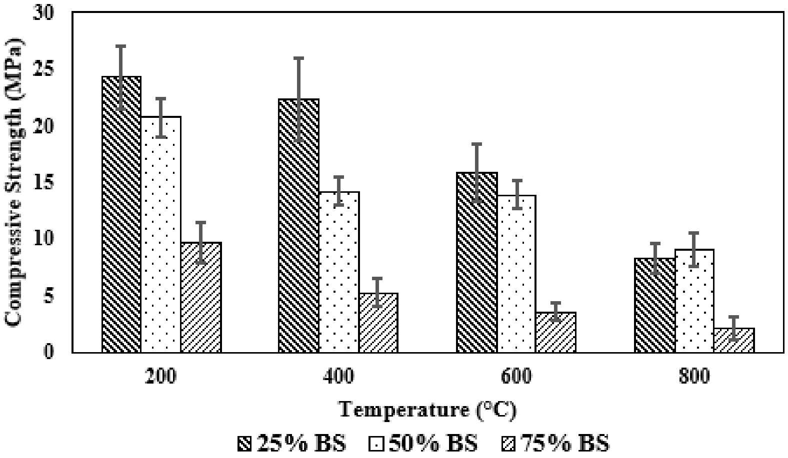

Fig. 9 Temperature Vs Compressive Strength Curve

However, at 14M, the compressive strength decreased due to the formation of surface cracks on the composites, as evident in **Fig. 8.** This reduction can be attributed to potential issues such as efflorescence or excessive shrinkage associated with higher NaOH concentrations, which compromise the structural integrity of the composites.

3.2.5 Thermal Exposure

The graph on **Fig. 9** shows the compressive strength of materials with 25%, 50%, and 75% BA at temperatures ranging from 100 ℃ to 800 ℃ with the variation shown on **Table 9**. Compressive strength decreases as temperature increases for all compositions. Materials with 25% BA exhibit the highest strength, starting above 25 MPa, while 75% BA shows the lowest, starting below 10 MPa. The decline is more pronounced at temperatures above 600 ℃, with all materials losing significant strength by 800 ℃. Lower BA content improves thermal resistance, making 25% BA the most mechanically stable under high temperatures.

Table 9. Composition Variation for Thermal Exposure Test

Parameter	Details
Composition	BS: FA Ratios- 25:75, 50:50
AA Ratio (Na_2SiO_3 /NaOH)	1.5
Solid-to-Liquid Ratio	1.5
Temperature (℃)	200, 400, 600, 800

Moreover, compressive strength subsequently decreases at higher temperatures due to thermal degradation. At higher temperatures loss of water of Hydration is a cause of that. Also, elevated temperatures influence the behavior of pozzolanic materials, with higher temperatures causing greater weight loss and a decrease in pozzolanic activity [42].

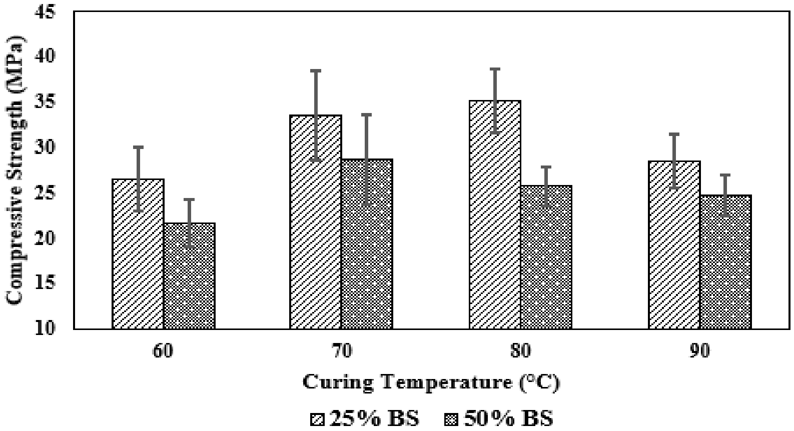

Fig. 10. Curing Temperature Variation Vs Compressive Strength Curve

3.2.6 Curing Temperatures Variation:

The graph on **Fig. 11** illustrates the compressive strength of materials with 25% and 50% BS as a function of curing temperature (℃), ranging from 60 ℃ to 90 ℃ with the variation shown on **Table 10.**

Table 10. Composition Variation for Curing Temperature

Parameter	Details
Composition	BS: FA Ratios- 25:75, 50:50
AA Ratio (Na_2SiO_3 /NaOH)	1.5
Solid-to-Liquid Ratio	1.5
Initial Oven Curing Temperature (℃) for 24 hours	60, 70, 80, 90

For both compositions, compressive strength initially increases with curing temperature, peaks between 70 ℃ and 80 ℃, and then declines at higher curing temperatures. Composites with 25% BS consistently exhibit higher compressive strength compared to those with 50% BS across all curing temperatures. The peak strength for the 25% BS composition is approximately 35.1 MPa at 70 ℃, while for the 50% BS composition, it reaches 28.69 MPa at 80 ℃.

At 90 ℃, the compressive strength declines for both compositions. This trend suggests that an optimal curing temperature enhances strength, but excessive curing temperatures beyond 80 ℃ led to degradation, likely due to microstructural changes, such as microcracking, or over-curing effects.

Additionally, the 50% BS composites have a higher porosity compared to the 25% BS composites, leading to greater water absorption. At lower curing temperatures, the excess water retained within the 50% BS composites may not fully escape, which could hinder the formation of a dense geopolymer matrix. In contrast, at higher curing temperatures, the evaporation of this excess water facilitates better geopolymerization, resulting in improved strength up to the optimal temperature.

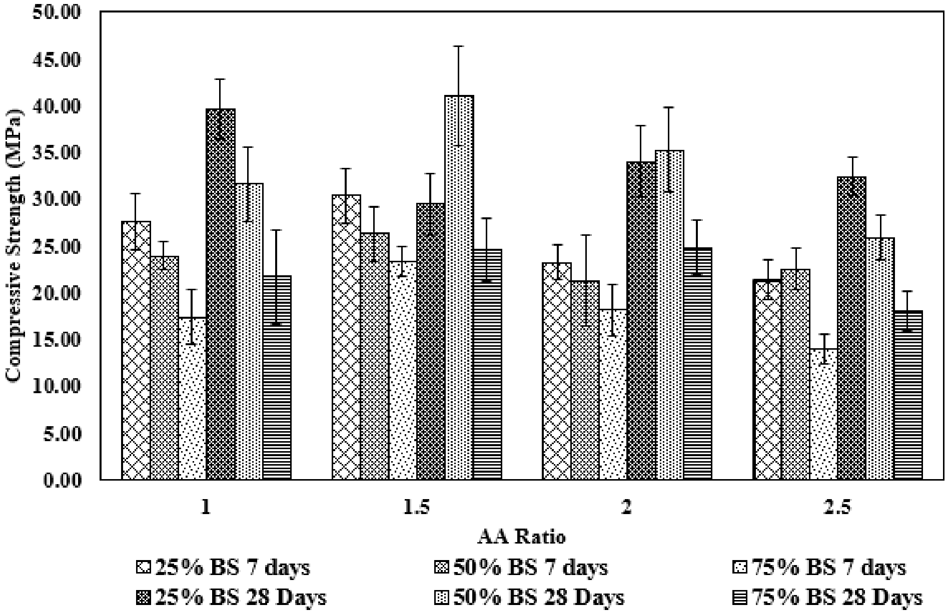

Fig. 11. Comparison of Compressive Strength after 7 and 28 Days Curing with Variation of AA ratio (*S*/*L* 2).

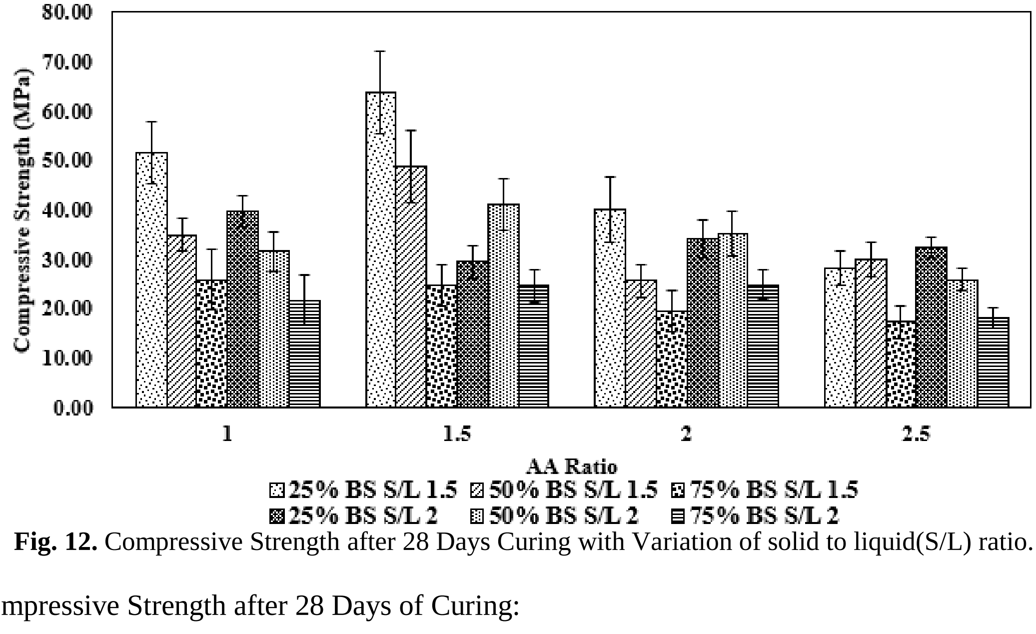

Fig. 12. Compressive Strength after 28 Days Curing with Variation of solid to liquid(S/L) ratio.

3.2.7 Compressive Strength after 28 Days of Curing:

The **Fig. 11** reveals that after 28 days of curing, the compressive strength increased for all variations. However, the extent of this increase varied; some showed significant improvement, while others exhibited only marginal gains. For those with limited strength development, the slower reaction kinetics could be a contributing factor. These composites may require extended curing periods to allow the alkali activator to fully react with the components of boiler slag and fly ash.

Coming to the graph on **Fig. 12** shows the compressive strength of materials with 25%, 50%, and 75% BS at varying alkali activator (AA) ratios and solid to liquid ratios (S/L = 2 and S/L = 1.5) for 28 days of curing. In all cases S/L=1.5 shows better results than S/L=2. This substantiates that for higher quantity of alkali-activator BS and FA particle to particle interaction is less and form a lower interparticle bond for long curing period also.

3.2.8 SEM Analysis:

The **Fig. 13(a)** reveals a heterogeneous microstructure characterized by spherical particles (likely FA particles) embedded in a matrix. The spherical particles, known as cenospheres, are remnants of FA and exhibit hollow or porous structures. The presence of holes **Fig. 13 (b)** in cenospheres can be attributed to the trapping and release of gases during the high-temperature combustion process. As coal particles burn in power plants, gases such as CO_2 and water vapor become trapped inside. When the droplets rapidly cool and solidify, these trapped gases escape, leaving voids or holes on the surface of the cenospheres [43].

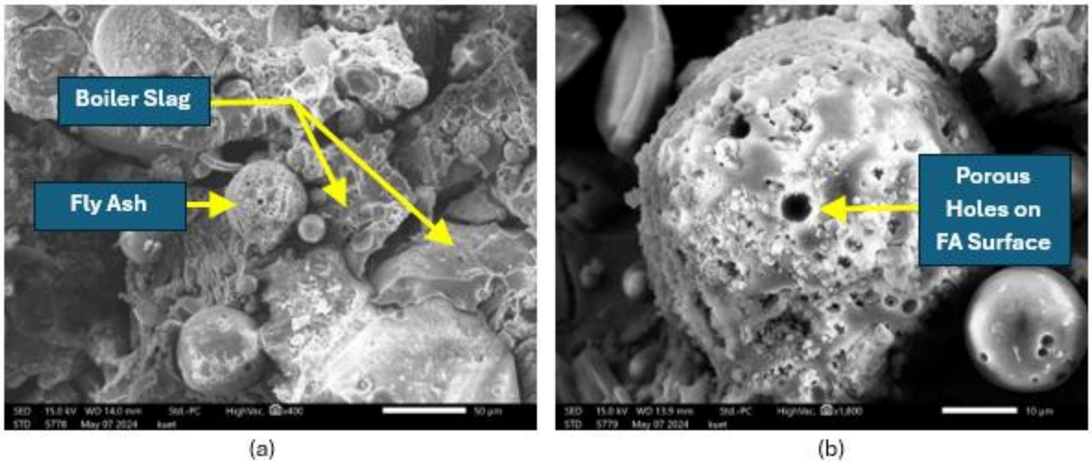

(a) (b)

Fig. 13. (a) SEM Analysis of 10M NaOH *S/L* ratio 1.5 and AA ratio 1.5 @75% BS, 70 ℃ curing temperature; (b) FA cenosphere after activated with AA @75% BS

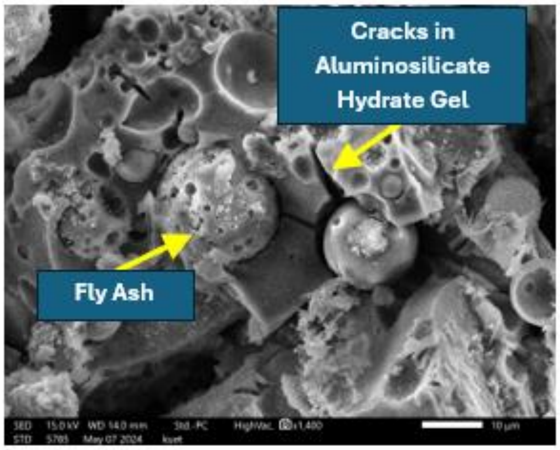

Fig. 14. SEM analysis after thermal exposure @200 ℃

BS tends to have irregular shapes and a denser structure, in the image **Fig. 14** **(a)**, the angular fragments or more compact-looking areas likely represent the contribution of BS. Some parts of the matrix exhibit amorphous or partially crystalline phases, suggesting the presence of geopolymerization products like sodium aluminosilicate hydrate (N-A-S-H) gel.

In **Fig. 14.** SEM analysis after thermal exposure @200 ℃ Micro-voids, cracks and pores are clearly visible comparing to **Fig.14 (a)**, which might influence the material's mechanical strength and durability on high temperature exposure.

4 Conclusion

The primary objective of this study was to explore sustainable alternatives of raw materials for conventional FAB manufacturing materials in order to enhance environmental performance. The results from this study demonstrate promising performance when compared to established international standards for FAB, such as ASTM C62, BA 3921, and IS 1077: 1992. Based on these results, it is proposed that BA and an AA can be used in FAB production. Which can be replacements for geo-sand and cement, offering an eco-friendlier solution for FAB production. This approach aligns with current trends in material science, which aim to reduce the environmental impact of traditional construction materials. Some Bullet findings are as follows:

1. Apparent porosity and water absorption decreases with an increase in BA content.
2. Optimal strength performance is observed with a 25% BA mixture and an AA ratio of 1.5.
3. Both S/L ratios of 1.5 and 2.0 are effective for the mixture.
4. A 10M NaOH concentration is ideal, as it results in fewer cracks in the final composite.
5. At higher temperatures, BA-mixed composites perform similarly to conventional composites.
6. Initial curing temperatures between 70°C and 80°C are optimal for the process.
7. After 28 days of curing, some composites show limited strength development, indicating the need for additional maturation time.
8. High temperature exposure causes internal cracking of alkali-activator crystals, reducing strength. Additionally, porous holes form on fly ash particles due to gas evacuation at elevated temperatures.

Acknowledgement

The authors sincerely express their gratitude to **Khulna University of Engineering & Technology (KUET)** for providing laboratory facilities and equipment for research. Appreciation is extended to **Bangladesh-India Friendship Power Company Limited (BIFPCL)** for supplying raw materials and to **Bharat Heavy Electricals Limited (BHEL)** for providing technical equipment support. Their collective contributions have been instrumental in advancing this study.

Funding Statement

The author(s) received no specific funding for this study.

Credit authorship contribution statement

Jasim Ahmed Chowdhury: Investigation, Formal analysis, Writing – original draft. **Md. Shahidul Islam**: Conceptualization, Supervision, Formal analysis, Writing – review & editing. **Md. Ashraful Islam**: Supervision, Writing – review & editing. **Md Abdullah Al Bari**: Supervision, Writing – review & editing, **Arup Kumar Debnath**: Investigation, Writing – review & editing.

Conflicts of Interest

The authors declare that they have no conflicts of interest to report regarding the present study.

Data Availability Statement

Some or all data, models, or codes that support the findings of this study are available from the corresponding author upon reasonable request.

References

[1] R. Kumar and N. Hooda. An experimental study on properties of fly ash bricks. International journal of research in aeronautical and mechanical engineering 2014; 2(9): 56-67.

[2] Imarcgroup, Fly Ash Market Size and Share. https://www.imarcgroup.com/fly-ash-market (accessed 16 November, 2024).

[3] G. I. Research, Global Fly Ash Bricks Market 2024 by Manufacturers, Regions, Type and Application,Forecast to 2030, 02 Jan 2024. https://www.globalinforesearch.com/reports/1750720/fly-ash-bricks (accessed: 17/12/2024)

[4] V. Reports, Global Fly Ash Bricks Market 2024 by Manufacturers, Regions, Type and Application, Forecast to 2030. 2024. https://reports.valuates.com/market-reports/QYRE-Auto-12H3634/global-fly-ash-bricks (accessed: Dec. 17, 2024).

[5] M. Priyadarshini, M. Patnaik, and J. P. Giri. A probabilistic approach for identification of compressive strength of fly ash bricks. Innovative Infrastructure Solutions 2018; 3(1). doi: 10.1007/s41062-018-0162-3.

[6] K. S. Devi, V. V. Lakshmi, and A. Alakanandana. Impacts of cement industry on environment-an overview. Asia Pac. J. Res 2017; 1: 156-161.

[7] M. Rafieizonooz, J. Mirza, M. R. Salim, M. W. Hussin, and E. Khankhaje. Investigation of coal bottom ash and fly ash in concrete as replacement for sand and cement. Construction and Building Materials 2016; 116: 15-24. doi: 10.1016/j.conbuildmat.2016.04.080.

[8] F. Rao and Q. Liu. Geopolymerization and Its Potential Application in Mine Tailings Consolidation: A Review. Mineral Processing and Extractive Metallurgy Review 2015; 36(6): 399-409. doi: 10.1080/08827508.2015.1055625.

[9] D. Khale and R. Chaudhary. Mechanism of geopolymerization and factors influencing its development: a review. Journal of Materials Science 2007; 42(3): 729-746. doi: 10.1007/s10853-006-0401-4.

[10] E. Benhelal, G. Zahedi, E. Shamsaei, and A. Bahadori. Global strategies and potentials to curb CO2 emissions in cement industry. Journal of cleaner production 2013; 51: 142-161. doi: https://doi.org/10.1016/j.jclepro.2012.10.049.

[11] A. Buchwald and M. Schulz. Alkali-activated binders by use of industrial by-products. Cement and concrete research 2005; 35(5): 968-973. doi: https://doi.org/10.1016/j.cemconres.2004.06.019.

[12] J. Davidovits. Geopolymers: inorganic polymeric new materials. Journal of Thermal Analysis and calorimetry 1991; 37(8): 1633-1656. doi: https://doi.org/10.1007/bf01912193.

[13] Our World in Data, Electricity Production by Source, World. https://ourworldindata.org/grapher/electricity-prod-source-stacked, (accessed 17 November, 2024).

[14] IEA, Executive Summury. https://www.iea.org/reports/coal-2023/executive-summary, (accessed 2024, 17/11).

[15] Bangladesh Power Development Board, Installed Capacity of BPDB Power Plants as on November 2024. https://misc.bpdb.gov.bd/power-generation-unit, (accessed 17 November, 2024).

[16] T. H. Adams, Coal Ash Recycling Rate Increased in 2022, Ash Harvesting Continued at Significant Volumes, December 27, 2023 2023.

[17] R. Hatt and K. Versailles. Understanding boiler slag. Coal combustion. Inc 1990, Versailles. 1:3.

[18] T. Zeng, A. Mlonka-Mędrala, V. Lenz, and M. Nelles. Evaluation of bottom ash slagging risk during combustion of herbaceous and woody biomass fuels in a small-scale boiler by principal component analysis. Biomass Conversion and Biorefinery 2021; 11: 1211-1229. doi: https://doi.org/10.1007/s13399-020-00607-2.

[19] Z.-m. Li, F.-z. Sun, L. Ma, W. Wei, and F. Li. Low-pressure economizer increases fly ash collection efficiency in ESP. Applied Thermal Engineering 2016; 93: 509-517. doi: 10.1016/j.applthermaleng.2015.10.006.

[20] Dr.R.Kumutha1, D. K. V. , S. N. N. , M. N. , and a. R. M. Preethi. Experimental Investigation on Fly Ash Bricks Incorporating M-Sand and GGBS. International Journal of Constructive Research in Civil Engineering 2018; 4(2). doi: 10.20431/2454-8693.0402001.

[21] P. S. M. S. Ravikumar. Bricks made with fly ash - A review of recent developments. AIP Conference Proceedings 2023. AIP Conf. Proc: 2690. doi: 10.1063/5.0061285.

[22] S. Naganathan, A. Y. O. Mohamed, and K. N. Mustapha. Performance of bricks made using fly ash and bottom ash. Construction and Building Materials 2015; 96: 576-580. doi: 10.1016/j.conbuildmat.2015.08.068.

[23] S. S. Djwantoro HARDJITO, FUNG. Fly Ash-Based Geopolymer Mortar Incorporating Bottom Ash. Modern Applied Science 2010; 4: 44-52.

[24] M. M. A. Abdullah, H. Kamarudin, M. Bnhussain, I. Khairul Nizar, A. R. Rafiza, and Y. Zarina. The Relationship of NaOH Molarity, Na2SiO3/NaOH Ratio, Fly Ash/Alkaline Activator Ratio, and Curing Temperature to the Strength of Fly Ash-Based Geopolymer. Advanced Materials Research 2011; 328-330: 1475-1482. doi: 10.4028/www.scientific.net/AMR.328-330.1475.

[25] S. Abdullah, L. Ming, M. Abdullah, H. Yong, and K. Zulkifly. Evaluation on mixing parameter of S/L and Na2SiO3/NaOH ratios towards fly ash geopolymers. AIP Conference Proceedings, 2018; 2030(1):AIP Publishing. doi: https://doi.org/10.1063/1.5066936.

[26] H. Y. Leong, D. E. L. Ong, J. G. Sanjayan, and A. Nazari. The effect of different Na2O and K2O ratios of alkali activator on compressive strength of fly ash based-geopolymer. Construction and Building Materials 2016; 106: 500-511. doi: https://doi.org/10.1016/j.conbuildmat.2015.12.141.

[27] M. N. Hadi, M. Al-Azzawi, and T. Yu. Effects of fly ash characteristics and alkaline activator components on compressive strength of fly ash-based geopolymer mortar. Construction and Building Materials 2018; 175: 41-54. doi: https://doi.org/10.1016/j.conbuildmat.2018.04.092.

[28] J. L. Provis, A. Palomo, and C. Shi. Advances in understanding alkali-activated materials. Cement and Concrete Research 2015; 78: 110-125. doi: https://doi.org/10.1016/j.cemconres.2015.04.013.

[29] O. Juntarasakul, P. Roongcharoen, C. B. Tabelin, and T. Phengsaart. Municipal Solid Waste Incineration (MSWI) Fly Ash as a Potential Adsorbent for Phosphate Removal. Sustainability 2014; 16(20), doi: 10.3390/su16208869.

[30] W. M. W. Ibrahim, M. M. A. B. Abdullah, R. Ahmad, M. F. M. Tahir, N. A. M. Mortar, and M. A. A. N. Azli. Mechanical and physical properties of bottom ash/fly ash geopolymer for pavement brick application. IOP Conference Series: Materials Science and Engineering, 2020; 743(1): 012029. doi: 10.1088/1757-899X/743/1/012029.

[31] A. A. Maghsoudi and H. A. Moghadam. Properties assessment of concrete containing Sirjan Pozzolan.KSCE Journal of Civil Engineering 2016; 20(5): 1863-1869. doi: 10.1007/s12205-015-0423-z.

[32] W.-T. Kuo and Z.-C. Gao. Engineering Properties of Controlled Low-Strength Materials Containing Bottom Ash of Municipal Solid Waste Incinerator and Water Filter Silt. Applied Sciences 2018; 8(8), doi: 10.3390/app8081377.

[33] S. Saloma, H. Hanafiah, D. O. Elysandi, and D. G. Meykan. Effect of Na2SiO3/NaOH on mechanicalproperties and microstructure of geopolymer mortar using fly ash and rice husk ash as precursor. AIP Conference Proceedings, 2017; 1903(1): AIP Publishing, doi: https://doi.org/10.1063/1.5011552.

[34] B. Nematollahi, J. Sanjayan, J. X. H. Chai, and T. M. Lu. Properties of fresh and hardened glass fiber reinforced fly ash based geopolymer concrete. key engineering materials 2104; 594: 629-633. doi: https://doi.org/10.4028/www.scientific.net/KEM.594-595.629.

[35] H. Y. Zhang, V. Kodur, B. Wu, J. Yan, and Z. S. Yuan. Effect of temperature on bond characteristics of geopolymer concrete. Construction and Building Materials 2018; 163: 277-285. doi: 10.1016/j.conbuildmat.2017.12.043.

[36] F. Aredes, T. Campos, J. Machado, K. Sakane, G. Thim, and D. Brunelli. Effect of cure temperature on the formation of metakaolinite-based geopolymer. Ceramics International 2015; 41(6): 7302-7311. doi: DOI: 10.1016/j.ceramint.2015.02.022.

[37] P. Pavithra, M. Srinivasula Reddy, P. Dinakar, B. Hanumantha Rao, B. Satpathy, and A. Mohanty. Effect of the Na2SiO3/NaOH ratio and NaOH molarity on the synthesis of fly ash-based geopolymer mortar. Geo-Chicago 2016; 2016: 336-344.

[38] M. Morsy, S. Alsayed, Y. Al-Salloum, and T. Almusallam. Effect of sodium silicate to sodium hydroxide ratios on strength and microstructure of fly ash geopolymer binder. Arabian journal for science and engineering 2014; 39: 4333-4339 2014. doi: https://doi.org/10.1007/s13369-014-1093-8.

[39] S. H. Park, H. S. Ryu, and W. J. Park. Influence of Unit Water Content Control on Concrete Performance in the Ready-Mixed Concrete Production Process (in eng). Materials (Basel) Feb 9 2024; 17(4), doi: 10.3390/ma17040834.

[40] P. Chindaprasirt, C. Jaturapitakkul, W. Chalee, and U. Rattanasak. Comparative study on the characteristics of fly ash and bottom ash geopolymers. Waste Manag Feb 2009; 29(2): 539-43. doi: 10.1016/j.wasman.2008.06.023.

[41] A. Sathonsaowaphak, P. Chindaprasirt, and K. Pimraksa. Workability and strength of lignite bottom ash geopolymer mortar. J Hazard Mater Aug 30 2009; 168(1): 44-50. doi: 10.1016/j.jhazmat.2009.01.120.

[42] I. Quadri and A. O. Bankole. The effect of elevated temperature on the performance of pozzolanic cement mortar. Discover Civil Engineering 2024; 1(1): 50. doi: 10.1007/s44290-024-00056-0.

[43] R. J. Lauf, Cenospheres in fly ash and conditions favouring their formation. Fuel 1981; 60(12): 1177-1179. doi:10.1016/0016-2361(81)90079-x.